



ORIGINAL ARTICLE

Genetic evidence implies that primary and relapsed tumors arise from common precursor cells in primary central nervous system lymphoma

Keiichiro Hattori^{1,2}  | Mamiko Sakata-Yanagimoto^{1,2} | Manabu Kusakabe^{1,2}  | Toru Nanmoku³ | Yasuhito Suehara^{1,2} | Ryota Matsuoka⁴ | Masayuki Noguchi⁴ | Yasuhisa Yokoyama^{1,2} | Takayasu Kato^{1,2} | Naoki Kurita² | Hidekazu Nishikii^{1,2} | Naoshi Obara^{1,2} | Shingo Takano⁵ | Eiichi Ishikawa⁵ | Akira Matsumura⁵ | Masafumi Muratani⁶ | Yuichi Hasegawa² | Shigeru Chiba^{1,2}

¹Department of Hematology, Graduate School of Comprehensive Human Sciences, University of Tsukuba, Tsukuba, Japan

²Department of Hematology, Faculty of Medicine, University of Tsukuba, Tsukuba, Japan

³Department of Clinical Laboratory, University of Tsukuba Hospital, Tsukuba, Japan

⁴Department of Pathology, Faculty of Medicine, University of Tsukuba, Tsukuba, Japan

⁵Department of Neurosurgery, Institute of Clinical Medicine, University of Tsukuba, Tsukuba, Japan

⁶Department of Genome Biology, Faculty of Medicine, University of Tsukuba, Tsukuba, Japan

Correspondence

Mamiko Sakata-Yanagimoto and Shigeru Chiba, Department of Hematology, Faculty of Medicine, University of Tsukuba, Tsukuba, Japan.

Emails: sakatama-tky@umin.net and schiba-tky@umin.net

Funding information

Ministry of Education, Culture, Sports, and Science of Japan, Grant/Award Number: 16H02660 and 18H02134; Kobayashi Foundation for Cancer Research; Leukemia Research Fund; Takeda Science Foundation for Cancer Research

Primary central nervous system lymphoma (PCNSL) is a rare subtype of lymphoma that arises within the brain or the eyes. PCNSL recurs within the central nervous system (CNS) in most relapsed cases, whereas extra-CNS relapse is experienced in rare cases. The present study aimed at identifying the presence of common precursor cells (CPC) for primary intra- and relapsed extra-CNS tumors, and further assessing the initiating events in bone marrow (BM). Targeted deep sequencing was carried out for five paired primary intra- and relapsed extra-CNS tumors of PCNSL. Two to five mutations were shared by each pair of intra- and extra-CNS tumors. In particular, *MYD88* mutations, L265P in three and P258L in one, were shared by four pairs. Unique somatic mutations were observed in all five intra-CNS tumors and in four out of five extra-CNS tumors. Remarkably, *IgH* clones in the intra- and the extra-CNS tumors in two pairs were distinct from each other, whereas one pair of tumors shared identical monoclonal *IgH* rearrangement. In a cohort of 23 PCNSL patients, L265P *MYD88* mutations were examined in tumor-free BM mononuclear cells (MNC) in which the PCNSL tumors had L265P *MYD88* mutations. L265P *MYD88* mutations were detected by a droplet digital PCR method in nine out of 23 bone marrow mononuclear cells. These results suggest that intra- and extra-tumors are derived from CPC with *MYD88* mutations in most PCNSL, arising either before or after *IgH* rearrangement. The initiating *MYD88* mutations may occur during B-cell differentiation in BM.

KEYWORDS

bone marrow, common precursor cell, *IgH* rearrangement, L265P *MYD88*, primary central nervous system lymphoma

This is an open access article under the terms of the Creative Commons Attribution-NonCommercial-NoDerivs License, which permits use and distribution in any medium, provided the original work is properly cited, the use is non-commercial and no modifications or adaptations are made.

© 2018 The Authors. *Cancer Science* published by John Wiley & Sons Australia, Ltd on behalf of Japanese Cancer Association.

1 | INTRODUCTION

Primary central nervous system lymphoma (PCNSL) is a rare form of diffuse large B-cell lymphoma (DLBCL) that arises within the brain or eyes.¹ Recent exome sequencing studies have shown that genes of the Toll-like receptor and B-cell receptor signaling pathways are frequently mutated in PCNSL.²⁻⁴ Notably, the hotspot mutation of *MYD88*, which results in the conversion from leucine to proline at the 265th position (L265P *MYD88* mutation), has a very high prevalence in patients with PCNSL (38%-85.4%).²⁻⁵

A previous report showed that the L265P *MYD88* mutation, but not other mutations, found in PCNSL tumors was detected in peripheral blood mononuclear cells (PBMC).³ This may imply that the L265P *MYD88* mutation may occur at the extra-central nervous system (CNS) compartment as the initial genetic event for PCNSL development. However, the actual developmental process of PCNSL should be examined from a different point of view.

Comparisons between genomic alterations in tumors at diagnosis and those at relapse led to the suggestion of common precursor cells (CPC) for the primary and relapsed tumors in other types of lymphoma such as follicular lymphomas (FL) and mantle cell lymphomas (MCL).^{6,7} Primary and relapsed tumors of FL and MCL may arise through a divergent evolution pattern from CPC by acquiring mutations specific to either primary or relapsed tumors.^{6,7} PCNSL recurs within the CNS in most relapsed cases, whereas extra-CNS relapse (systemic relapse) is experienced in <7% of the relapsed cases.¹ The present study aimed at identifying the presence of CPC with multiple mutations by examining paired primary intra- and relapsed extra-CNS tumors and further assessing the initiating events by examining *MYD88* mutations in bone marrow mononuclear cells (BMMNC).

2 | MATERIALS AND METHODS

2.1 | Targeted deep sequencing by Ion Torrent PGM

Targeted deep sequencing (TDS) was carried out in five paired primary intra-CNS and relapsed extra-CNS tumors and BMMNC using the Lymphopanel for 34 candidate genes⁸ and our in-house PCNSL panel for 12 candidate genes¹ (Tables S1 and S2). Because seven genes overlapped, 39 candidate genes were analyzed in total. The mutational profiles of five primary intra-CNS tumors by our in-house PCNSL panel were previously described.¹ Both panels were designed by custom Ampliseq Designer system (Thermo Fisher Scientific, Waltham, MA, USA). Libraries were prepared from 5 ng tumor DNAs using the Ion AmpliSeq Library Kit 2.0 (Thermo Fisher Scientific), according to the manufacturer's instructions. Sequencing was carried out using Ion 318 chips on Ion Torrent Personal Genome Machine (PGM) (Thermo Fisher Scientific). Data were analyzed by carrying out alignment with the hg19 human reference genome and variant calling was done with Variant Caller 5.2 (Thermo Fisher Scientific). Single nucleotide variants or insertions/deletions with frequencies of 3% or more were considered candidate mutations.

These mutations were validated by genomic PCR followed by Sanger sequencing. The primers are listed in Table S3.

2.2 | Polymerase chain reaction detection of complementarity-determining region 3 region of Ig heavy chain genes

Polymerase chain reaction (PCR) for amplification of the complementarity-determining region 3 (CDR3) was carried out in a semi-nested approach.⁹ The first step of PCR was carried out using primer FR2A or FR3A plus a reverse primer directed at the joining region (LJH). In the second step, the same forward primer (FR2A or FR3A) was used in mixtures with an inner reverse primer VLJH. The following primers were used: FR2A, TGGRTCCGMCAGSCYYCNGG; FR3A, ACACGGCYSTGTATTACTGT; LJH, TGAGGAGACGGTGACC; VLJH, GTGACCAGGGTNCCTTGCCCCAG. In both steps, the PCR mixture contained TaKaRa Taq reagents (Takara, Shiga, Japan). The first PCR (35 cycles) contained 100 ng DNA and the second PCR (20 cycles) contained 1 μ L of the undiluted first PCR product. The standard PCR cycle condition of the first step consisted of denaturation at 94°C for 15 seconds, annealing at 55°C for 30 seconds, and extension at 72°C for 30 seconds. The PCR cycle of the second step consisted of denaturation at 94°C for 10 seconds, annealing at 55°C for 10 seconds, and extension at 72°C for 10 seconds. These reactions were preceded by an initial denaturation step at 94°C for 5 minutes and concluded by a final extension at 72°C for 7 minutes. PCR products (10 μ L) were analyzed on 3% agarose gel stained with ethidium bromide by electrophoresis and viewed under ultraviolet light. Additionally, to improve resolution, PCR products were also run on acrylamide gel.

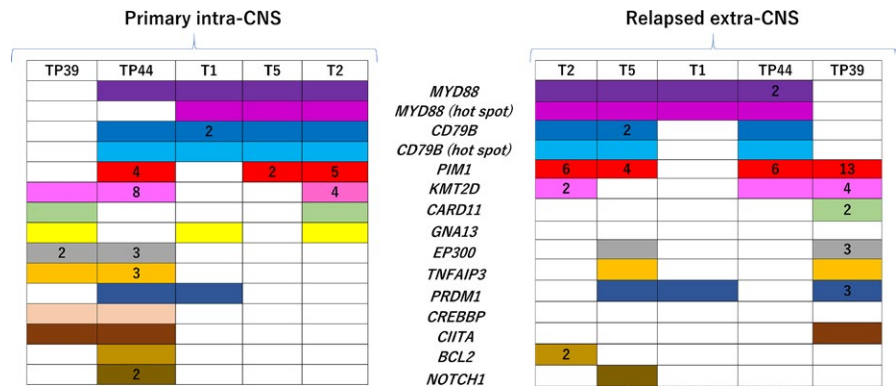
PCR amplicons were extracted by using QIAquick Gel Extraction Kit (Qiagen, Hilden, Germany) and sequenced by direct sequencing. Obtained sequences were analyzed using IMGT/V-QUEST from the international ImMunoGeneTics information system (IMGT) (<http://www.imgt.org>).¹⁰

3 | RESULTS

3.1 | Clinical features and quality evaluation of tumor samples

Clinical and histological findings of five PCNSL patients who experienced extra-CNS relapse are summarized in Tables S4 and S5. In all five patients, first complete response (CR) was achieved during or at the end of the modified European Organisation for Research and Treatment of Cancer (EORTC) chemotherapy for PCNSL⁴ and was maintained for more than 1 year (Figure S1). Subsequently, extra-CNS relapse occurred (Figure S1). Median time from diagnosis of PCNSL to extra-CNS relapse was 18 months (Table S4). Sites of extra-CNS relapse were maxillary sinus and submandibular lymph nodes in patient T1, intra-abdominal lymph nodes and subcutaneous tissue of back in T2, subcutaneous tissue of right thigh in T5, left breast, and left supraclavicular and intra-abdominal lymph nodes in TP39, and subcutaneous tissue of lower back

FIGURE 1 Recurrently mutated genes with primary central nervous system lymphoma (PCNSL). Comparison of mutated genes between primary or relapsed extra-central nervous system tumors of PCNSL. Numbers of mutations are indicated when more than one mutation was detected in the genes



and submandibular lymph nodes in TP44 (Table S4). All five patients had no detectable lesions in the CNS at the time of diagnosis of extra-CNS relapse. However, in one patient (patient T1), magnetic resonance imaging (MRI) findings confirmed CNS relapse in the left frontal lobe and the left optic nerve 1 month after diagnosis of extra-CNS relapse (Figure S1). Tumor cell content of each primary intra-CNS and relapsed extra-CNS tumor sample varied from 1.09% to 90% in flow cytometric or histological analysis (Table S6). Quality of the extracted DNA from tumor samples was described as $\Delta\Delta\text{CT}$ based on the results of real-time quantitative PCR by using Agilent FFPE QC Kit (Agilent, Wilmington, USA) (Data S1). $\Delta\Delta\text{CT}$ of paired tumor samples varied from 0.01 to 0.76 (Table S7).

3.2 | Recurrently mutated genes in PCNSL patients

Targeted deep sequencing was carried out for 39 genes in five tumor pairs using the Lymphopanel⁸ and our in-house PCNSL panel.⁴ Mean coverages in each panel were $1593 \times$ (range, 370–3099) and $1563 \times$ (range, 1084–1990), respectively. In primary intra-CNS tumors, 61 probable somatic mutations were identified including 53 nonsilent single nucleotide variants (SNV), seven deletions, and one insertion. Recurrent gene mutations were found in these such as *MYD88* (4/5), *CD79B* (4/5), *PIM1* (3/5), *KMT2D* (3/5), and *GNA13* (3/5). The mutation profile of intra-CNS tumors in our study was consistent with that of PCNSL in a previous report, in which the same Lymphopanel was used.¹¹ In relapsed extra-CNS tumors, 68 probable somatic mutations were identified including 57 nonsilent SNV, eight deletions, and three insertions. Genes such as *MYD88* (4/5), *CD79B* (3/5), *PIM1* (4/5), *KMT2D* (3/5), and *PRDM1* (3/5) were recurrently mutated (Figure 1; Table S8). An aberrant somatic hypermutation (aSHM) indicator value was calculated according to the algorithm of Khodabakhshi et al.¹² The value was lower than 0.1, showing that *PIM1* mutations were associated with aSHM (Data S1, Table S9).¹²

3.3 | Landscape of somatic mutations in primary intra- and relapsed extra-CNS tumors of PCNSL patients

We found shared mutations in all five paired tumors and unique mutations in all five intra-CNS tumors and in four out of five extra-CNS tumors (Figure 2). In total, 16 mutations in 11 genes

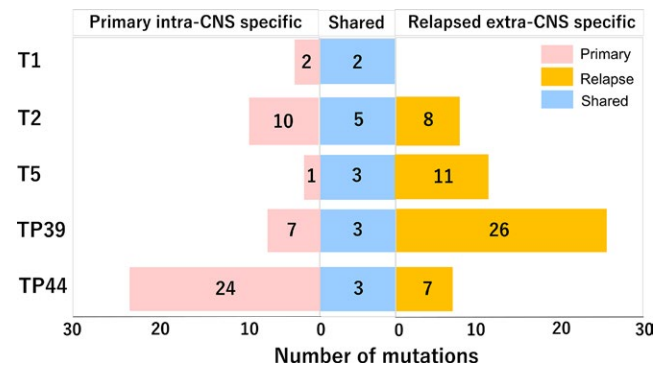


FIGURE 2 Number of somatic variants in each primary central nervous system (CNS) lymphoma tumor sample. Targeted deep sequencing for 39 genes was carried out for five paired tumors. Number of mutations found in both tumors (shared mutations), those specific to primary intra-CNS tumors, and those specific to extra-CNS tumors is indicated

were found to be shared (Figures 2 and 3; Table S8). *MYD88* (4/5) mutations, L265P in three and P258L in one, were the most recurrently shared mutations. *CD79B* (3/5), *KMT2D* (3/5), and *PIM1* (2/5) mutations also emerged as recurrently shared mutations, among which Y196 *CD79B* (3/5), and Q2951R *KMT2D* (2/5) were identified as hotspot mutations (Figure 1, Table S8). Forty-five mutations in six genes, including recurrent *GNA13* and *CREBBP* mutations were specific to primary intra-CNS tumors. (Figures 2 and 3; Figure S2, Table S8). Fifty-two mutations in six genes were specific to relapsed extra-CNS tumors (Figures 2 and 3; Figure S2, Table S8).

3.4 | Divergent evolution of primary intra- and relapsed extra-CNS tumors from a CPC

These distribution patterns of shared and separated mutations strongly indicated the presence of CPC that precedes the development of primary intra-CNS tumors. To seek the localization of the CPC in the B-lineage cell differentiation map, *IgH* rearrangement status of paired tumors was examined in paired tumors of patients T1, T5, and TP39 (Figures 4 and 5). PCR products of the CDR3 region of *IgH* showed a single sharp band the same size in both intra- and extra-CNS tumors of

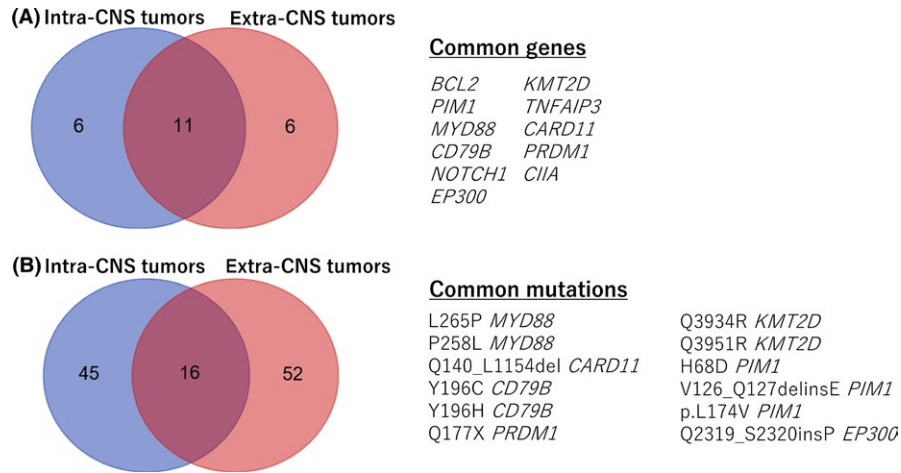


FIGURE 3 Overlaps in genes and somatic mutations discovered in intra- and extra-central nervous system (CNS) tumors. Venn diagram shows the comparison of genes and mutations between five intra- and extra-CNS tumor samples (A) Mutated genes shared between intra- and extra-CNS tumors were shown in overlap of the venn diagram. Detail of shared mutated genes were written under “Common genes”. (B) Somatic mutations shared between intra- and extra-CNS tumors were shown in overlap of the venn diagram. Detail of shared mutations were written under “Common mutations”.

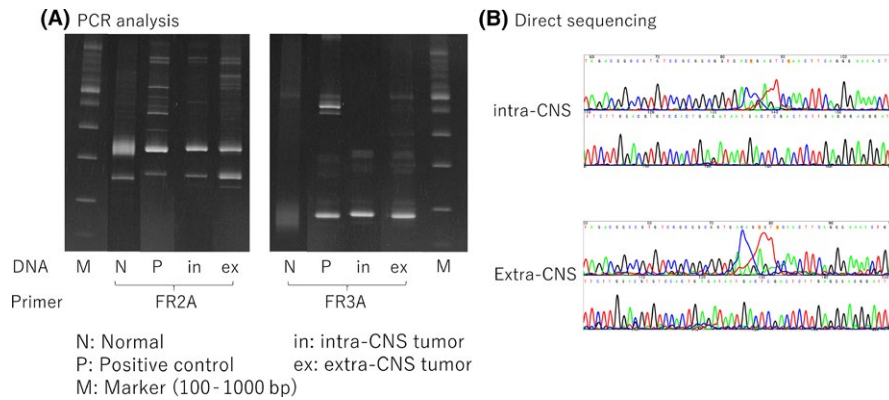


FIGURE 4 *IgH* rearrangement status of paired tumors in patient T1. (A) Photographs of PCR gels and (B) the electropherogram of direct sequencing show the *IgH* rearrangement status of paired tumors in patient T1. CNS, central nervous system

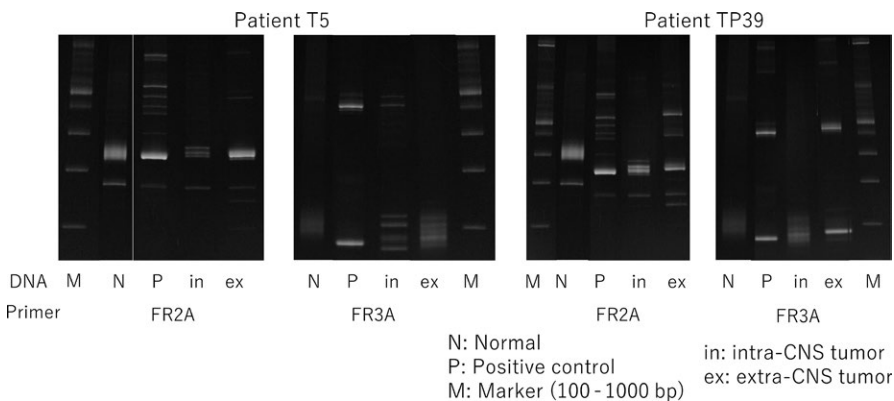
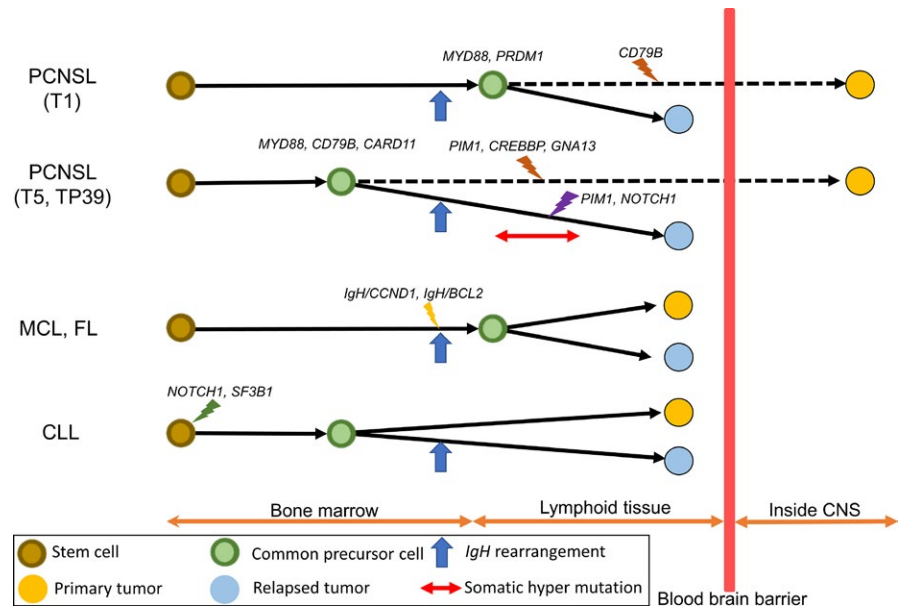


FIGURE 5 PCR analysis of *IgH* rearrangement status of paired tumors in patients T5 and TP39. Photographs of PCR gels show the *IgH* rearrangement status of paired tumors in patients T5 and TP39. CNS, central nervous system

patient T1 (Figure 4). Direct sequencing of the clonal bands confirmed that both tumors shared identical CDR3 sequences (Figure 4). In contrast, multiple bands were observed in the intra-CNS tumors of patient T5 and TP39, whereas the extra-CNS tumor of each patient appeared to have a single band (Figure 5). CDR3 sequences of both extra-CNS

and intra-CNS tumors of patients T5 and TP39 could not be determined by direct sequencing. Then, the PCR products were cloned into a plasmid and each clone recovered from *Escherichia coli* colonies was sequenced to determine the clonality. Variable regions of *IgH* (VH) were derived from either the V_H3 or V_H4 family in both tumors of T5 (Table



S10). Nevertheless, the CDR sequences were mostly mapped to the VH genes of the V_H3 family (V_H3-23^*04 , $V3-72^*01$, or $V3-30-3^*03$) in the intra-CNS tumor, whereas V_H4-4^*07 of the V_H4 family was dominant in the extra-CNS tumor (intra-CNS tumor, V_H3 16/18 [89%] vs V_H4 2/18 [11%]; extra-CNS tumor, V_H3 3/17 [18%] vs V_H4 14/17 [82%]) (Table S10). In TP39, VH were derived from the V_H4-4^*07 of the V_H4 family in the intra-CNS tumor, whereas V_H3-21^*01 of the V_H3 family was detected in the extra-CNS tumor (intra-CNS tumor, V_H3 1/17 [6%] vs V_H4 16/17 [94%] extra-CNS tumor, V_H3 18/18 [100%] vs V_H4 0/100 [0%]) (Table S10). Homology with the germline sequence and usage of $V_H-D_H-J_H$ genes are summarized in Table S10 and Figure S3. Predominantly repeated or similar clones with identical V-D-J usage were identified in all tumor samples. In T5 intra-CNS tumor, clones with $V_H3-23^*01/D_H4-23^*01/J_H6^*02$ rearrangement and those with $V_H3-72^*01/D_H6-25^*01/J_H6^*03$ rearrangement were identified dominantly in 4/18 [22%] and 4/18 [22%] (Table S10). In T5 extra-CNS tumor, clones with $V_H4-4^*07/D_H5-24^*01/J_H4^*01$ were dominantly identified in 14/17 [82%], in TP39 intra-CNS tumor, those with $V_H4-4^*07/D_H5-24^*01/J_H4^*01$ in 16/17 [94%] and in TP39 extra-CNS tumor, those with $V_H3-21^*01/D_H6-19^*01/J_H4^*01$ in 15/18 [83%] (Table S10). Almost all V_H were highly mutated (T5 intra-CNS tumor, 17/18; T5 extra-CNS tumor, 14/17; TP39 intra-CNS tumor, 16/17; TP39 extra-CNS tumor, 18/18) presumably because of ongoing hypermutation¹³⁻¹⁶ (Table S10, Figure S3).

These analyses imply that the CPC is mapped at distinct positions in B-lineage differentiation; the position after *IgH* rearrangement and even after hypermutation at the variable region was suggested in T1, whereas emergence of CPC before *IgH* rearrangement was suggested in T5 and TP39.

3.5 | Detection of L265P MYD88 mutations in BMMNC or PBMNC with droplet digital PCR

To further characterize the initiation of PCNSL that is theorized to precede the emergence of CPC, we analyzed PBMNC of T1 collected

at the diagnosis of extra-CNS relapse and BMMNC of T1, T2, T5 and 20 PCNSL patients in an extended cohort collected at diagnosis (N = 24). These 24 cases were those in whom the L265P MYD88 mutations were identified in primary PCNSL tumors. According to the pathological diagnosis, no clinical evidence of lymphoma infiltration was found in the bone marrow (BM) of these patients. The L265P MYD88 mutations were identified in PBMNC (T1) and in nine out of 23 BMMNC (in total, 10 of 24) by droplet digital PCR (ddPCR), whereas the mutations were not detected in any of the samples by TDS, a less sensitive method (Figure S4, Table S11).

4 | DISCUSSION

This is the first multidimensional study of mutational dynamics comparing mutational profiles between intra-CNS tumors and extra-CNS tumors. In our study, all the five paired tumors shared multiple mutations. Unique somatic mutations were observed in all the five intra-CNS tumors and four out of five extra-CNS tumors (Table S8, Figure S2). Among the somatic mutations specific to intra-CNS tumors, *TBL1XR1* mutation was reported to be more prevalent in PCNSL than in DLBCL not otherwise specified (NOS).¹⁷ In contrast, a *SOCS1* mutation was detected in the tumor of subcutaneous tissue in TP44 (Table S4). *SOCS1* mutations are known to be more prevalent in primary cutaneous diffuse large B-cell lymphoma, leg type compared to DLBCL NOS.¹⁸ Therefore, somatic mutations in these genes may bias the location of tumors. These results suggest that the paired tumors originate from divergent evolution of CPC through accumulation of distinct mutations.

Recent studies have proposed that primary and relapsed tumors in several hematological cancers may arise from CPC.^{6,7,18-20} Previously, it was reported that the dominant clones were identical in paired tumors of primary and relapsed MCL and FL according to the VDJ coding joints, suggesting that CPC may arise after

VDJ rearrangement (Figure 6).^{6,7} In contrast, in a part of Richter syndrome, distinct *IgH* clones were observed between aggressive lymphomas and primary chronic lymphocytic leukemia (CLL) tumors suggesting that divergence may occur before the VDJ rearrangements.^{19,20} In the current study, the existence of identical monoclonal B-cell clones in both intra- and extra-CNS tumors of T1 suggests that divergence from CPC could occur after the point of *IgH* rearrangement, similar to the case of FL and MCL (Figure 6). In contrast, distinct *IgH* clones were observed in the intra- and extra-CNS tumors of patients T5 and TP39, which suggests that divergence of CPC could occur preceding a VDJ rearrangement in BM, similar to the case of Richter syndrome in CLL (Figure 6).^{19,20} In a previous analysis, tumor-related *IgH* clones were detected in blood and bone marrow of three PCNSL patients.²¹ These results suggest that divergence from the CPC could occur after the point of *IgH* rearrangement in all of these patients, although hypermutations occurred independently in *IgH* clones of primary tumors in the CNS and in those in the systemic sites.²¹ This pattern is similar to the case of patient T1 in our study in which identical monoclonal B-cell clones existed in both intra- and extra-CNS tumors, although independent hypermutations were not observed in these tumors. In contrast, the findings in patients T5 and TP39 were remarkable because VDJ usage was different between intra- and extra-CNS tumors in these two patients.

It has been suggested that, in FL and MCL, the initial genetic events may occur in pre-B stage of differentiation during the recombination of the VDJ segments in the BM because the tumor cells harbor *IgH* fusions with other genes: *IgH/BCL2* in FL and *IgH/CCND1* in MCL. In several types of lymphomas, the initiating events could be tracked back even to hematopoietic stem/progenitor cells upstream of the lineage commitment towards either B cells or T cells: *NOTCH1* and *SF3B1* mutations in CLL,²² *BRAF* mutations in hairy cell leukemia²³ and *TET2/DNMT3A* mutations in angioimmunoblastic T-cell lymphomas.²⁴⁻²⁶ Frequent detection of L265P *MYD88* mutation in BM suggests that, in PCNSL patients, this mutation may occur before or during the B-cell differentiation process before the cells leave the BM environment and migrate to the peripheral lymphoid organs as naïve mature B lymphocytes. This theory, however, needs further proof because the presence of minimal contamination of lymphoma cells in the BM was not completely excluded in our study, although the presence of lymphoma cells was excluded by immunohistochemical evaluation and flow cytometry. Additionally, we were unable to examine the L265P *MYD88* mutation in healthy individuals. The L265P *MYD88* mutation was detected in PBMNC of only one subject at a mutation allele frequency of 23% in a cohort of 12 380 patients with psychiatric disease.²⁷ This mutation was undetected in that of any subject in another large cohort of 17 182 individuals without hematological malignancies.²⁸ Because the cutoff levels of mutation allele frequencies in both studies were 2%, smaller allele frequencies could have escaped detection and, therefore, the possibility cannot be completely excluded that very few cells with L265P *MYD88* are present even in healthy individuals.

In conclusion, our data suggest that intra- and extra-CNS tumors might originate from the CPC in PCNSL. The initial event could be

a mutation in the *MYD88* gene, and the emergence of CPC might follow by acquisition of subsequent genetic alterations. Precise clarification of these steps may contribute to establishing more robust biomarkers and therapeutic approaches with newly developed targeted drugs.

ACKNOWLEDGMENTS

This work was supported by Grants-in-Aid for Scientific Research (16H02660 to S.C. and 18H02134 to M.S.-Y.) from the Ministry of Education, Culture, Sports, and Science of Japan. This research was also partially supported by the Kobayashi Foundation for Cancer Research, Leukemia Research Fund and Takeda Science Foundation for Cancer Research to M.S.-Y.

CONFLICTS OF INTEREST

Authors declare no conflicts of interest for this article.

ORCID

Keiichiro Hattori  <http://orcid.org/0000-0002-0810-7887>

Manabu Kusakabe  <http://orcid.org/0000-0003-2518-0776>

REFERENCES

- Ferreri AJ, Reni M. Primary central nervous system lymphoma. *Crit Rev Oncol Hematol*. 2007;63:257-268.
- Bruno A, Boisselier B, Labreche K, et al. Mutational analysis of primary central nervous system lymphoma. *Oncotarget*. 2014;5:5065-5075.
- Fukumura K, Kawazu M, Kojima S, et al. Genomic characterization of primary central nervous system lymphoma. *Acta Neuropathol*. 2016;131:865-875.
- Hattori K, Sakata-Yanagimoto M, Okoshi Y, et al. *MYD88* (L265P) mutation is associated with an unfavourable outcome of primary central nervous system lymphoma. *Br J Haematol*. 2017;177:492-494.
- Taoka K, Okoshi Y, Sakamoto N, et al. A nonradiation-containing, intermediate-dose methotrexate regimen for elderly patients with primary central nervous system lymphoma. *Int J Hematol*. 2010;92:617-623.
- Pasqualucci L, Khiabani H, Fangazio M, et al. Genetics of follicular lymphoma transformation. *Cell Rep*. 2014;6:130-140.
- Wu C, de Miranda NF, Chen L, et al. Genetic heterogeneity in primary and relapsed mantle cell lymphomas: impact of recurrent *CARD11* mutations. *Oncotarget*. 2016;7:38180-38190.
- Dubois S, Viailly PJ, Mareschal S, et al. Next-generation sequencing in diffuse large B-cell lymphoma highlights molecular divergence and therapeutic opportunities: a LYSA study. *Clin Cancer Res*. 2016;22:2919-2928.
- Aiello A, Delia D, Giardini R, et al. PCR analysis of *IgH* and *BCL2* gene rearrangement in the diagnosis of follicular lymphoma in lymph node fine-needle aspiration. A critical appraisal. *Diagn Mol Pathol*. 1997;6:154-160.
- Brochet X, Lefranc M-P, Giudicelli V. IMGT/V-QUEST: the highly customized and integrated system for IG and TR standardized V-J and V-D-J sequence analysis. *Nucleic Acids Res*. 2008;36:W503-W508.
- Fontanilles M, Marguet F, Bohers E, et al. Non-invasive detection of somatic mutations using next-generation sequencing in primary

- central nervous system lymphoma. *Oncotarget*. 2017;8:48157-48168.
12. Khodabakhshi AH, Morin RD, Fejes AP, et al. Recurrent targets of aberrant somatic hypermutation in lymphoma. *Oncotarget*. 2012;3:1308-1319.
 13. Montesinos-Rongen M, Kuppers R, Schluter D, et al. Primary central nervous system lymphomas are derived from germinal-center B cells and show a preferential usage of the V4-34 gene segment. *Am J Pathol*. 1999;155:2077-2086.
 14. Thompsett AR, Ellison DW, Stevenson FK, Zhu D. V(H) gene sequences from primary central nervous system lymphomas indicate derivation from highly mutated germinal center B cells with ongoing mutational activity. *Blood*. 1999;94:1738-1746.
 15. Sekita T, Tamaru JI, Kaito K, Katayama T, Kobayashi M, Mikata A. Primary central nervous system lymphomas express Vh genes with intermediate to high somatic mutations. *Leuk Lymphoma*. 2001;41:377-385.
 16. Pels H, Montesinos-Rongen M, Schaller C, et al. VH gene analysis of primary CNS lymphomas. *J Neurol Sci*. 2005;228:143-147.
 17. Gonzalez-Aguilar A, Idbaih A, Boisselier B, et al. Recurrent mutations of MYD88 and TBL1XR1 in primary central nervous system lymphomas. *Clin Cancer Res*. 2012;18:5203-5211.
 18. Mareschal S, Pham-Ledard A, Viailly PJ, et al. Identification of somatic mutations in primary cutaneous diffuse large B-cell lymphoma, leg type by massive parallel sequencing. *J Invest Dermatol*. 2017;137:1984-1994.
 19. Mao Z, Quintanilla-Martinez L, Raffeld M, et al. IgVH mutational status and clonality analysis of Richter's transformation: diffuse large B-cell lymphoma and Hodgkin lymphoma in association with B-cell chronic lymphocytic leukemia (B-CLL) represent 2 different pathways of disease evolution. *Am J Surg Pathol*. 2007;31:1605-1614.
 20. Rossi D, Spina V, Deambrogi C, et al. The genetics of Richter syndrome reveals disease heterogeneity and predicts survival after transformation. *Blood*. 2011;117:3391-3401.
 21. McCann KJ, Ashton-Key M, Smith K, Stevenson FK, Ottensmeier CH. Primary central nervous system lymphoma: tumor-related clones exist in the blood and bone marrow with evidence for separate development. *Blood*. 2009;113:4677-4680.
 22. Landau DA, Tausch E, Taylor-Weiner AN, et al. Mutations driving CLL and their evolution in progression and relapse. *Nature*. 2015;526:525-530.
 23. Chung SS, Kim E, Park JH, et al. Hematopoietic stem cell origin of BRAFV600E mutations in hairy cell leukemia. *Sci Transl Med*. 2014;6:238ra71.
 24. Couronne L, Bastard C, Bernard OA. TET2 and DNMT3A mutations in human T-cell lymphoma. *N Engl J Med*. 2012;366:95-96.
 25. Sakata-Yanagimoto M, Enami T, Yoshida K, et al. Somatic RHOA mutation in angioimmunoblastic T cell lymphoma. *Nat Genet*. 2014;46:171-175.
 26. Nguyen TB, Sakata-Yanagimoto M, Nakamoto-Matsubara R, et al. Double somatic mosaic mutations in TET2 and DNMT3A—origin of peripheral T cell lymphoma in a case. *Ann Hematol*. 2015;94:1221-1223.
 27. Genovese G, Kahler AK, Handsaker RE, et al. Clonal hematopoiesis and blood-cancer risk inferred from blood DNA sequence. *N Engl J Med*. 2014;371:2477-2487.
 28. Jaiswal S, Fontanillas P, Flannick J, et al. Age-related clonal hematopoiesis associated with adverse outcomes. *N Engl J Med*. 2014;371:2488-2498.

SUPPORTING INFORMATION

Additional supporting information may be found online in the Supporting Information section at the end of the article.

How to cite this article: Hattori K, Sakata-Yanagimoto M, Kusakabe M, et al. Genetic evidence implies that primary and relapsed tumors arise from common precursor cells in primary central nervous system lymphoma. *Cancer Sci*. 2019;110:401–407. <https://doi.org/10.1111/cas.13848>